2013

Dressed Return Maps Distinguish Chaotic Mechanisms

Daniel J. Cross
Haverford College, dcross@haverford.edu

Dressed return maps distinguish chaotic mechanisms

Daniel J. Cross
Physics Department, Haverford College, Haverford, Pennsylvania 19041, USA

R. Gilmore
Physics Department, Drexel University, Philadelphia, Pennsylvania 19104, USA

(Received 8 October 2012; published 31 January 2013)

Chaotic data generated by a three-dimensional dynamical system can be embedded into $\mathbb{R}^3$ in a number of inequivalent ways. However, when lifted into $\mathbb{R}^5$ they all become equivalent, indicating that they all belong to a single universality class sharing a common chaos-generating mechanism. We present a complete invariant determining this universality class and distinguishing attractors generated by distinct mechanisms. This invariant is easily computable from an appropriately "dressed" return map of any particular three-dimensional embedding.

DOI: 10.1103/PhysRevE.87.012919 PACS number(s): 05.45.Ac, 02.20.−a, 02.40.Pc

I. INTRODUCTION

A major aim for the analysis of data generated by chaotic dynamical systems is determining the chaos-generating mechanism. Typical techniques attempt to reconstruct the original dynamics through an embedding of the data [1–5], but different embedding procedures can lead to different embeddings [6–9]. Topological analysis [5] provides information about the mechanism, but in an embedding-dependent way. In this paper, we present a method that, although built on topological analysis, is embedding-independent and so uniquely determines the chaos-generating mechanism. We consider only genus-1 attractors in detail; higher genus attractors will be treated in a forthcoming manuscript.

The spectrum of all possible embeddings for dissipative three-dimensional dynamical systems is now known [9–12]. Embeddings are distinguished by three degrees of freedom that describe the suspension flow between the various components of the Poincaré surface of section: global torsion, knot type, and parity. Since the embedding freedom resides in the suspension, this suggests that the mechanism can be determined by the return map alone. While this is not possible using the bare one-dimensional return maps possessed by dissipative systems (see, e.g., Fig. 2), it becomes possible if we "dress" the return map with additional information. We define these dressed return maps in Sec. II. In Sec. III, we show that any two dressed return maps describing the same mechanism are related by a group action. In Sec. IV, we introduce a complete invariant for determining mechanisms by modding out this group, and we compute several examples. We summarize our results in Sec. V.

II. DRESSED RETURN MAPS

Every embedding of a genus-1 attractor (e.g., the Rössler attractor [13]) is bounded by the surface of a torus of genus 1 [14]. A Poincaré surface of section can be chosen as a disk that is everywhere transverse to the flow. By the Birman-Williams theorem [4,5,15,16], the flow can be projected onto a two-dimensional branched manifold within the torus. The number of branches is equal to the number of symbols required to uniquely specify all trajectories. The Poincaré section can always be chosen to include the branch line, which is where all of the branches of the branched manifold are joined. The branched manifold can be described algebraically by (i) an integer index labeling each branch, (ii) the number of twists that each branch makes in the return trip to the branch line, and (iii) the order in which the different branches join when approaching the branch line. The return map for the flow only indicates the connectivity (and relative orientations) of the branches, but can be dressed to include the above information describing the branched manifold.

We dress each of the n branches in the return map with three symbols analogous to those describing the branched manifold. The first symbol i is the name of the branch: $i = 0, 1, \ldots, n-1$. The labeling is sequential from one end of the branch line to the other. The order of the labeling involves a choice, equivalent to choosing an orientation of the branch line. Once an orientation is given, the labeling is uniquely determined by continuity and adjacency (e.g., branch 2 is adjacent to branches 1 and 3). A conventional choice is to order the branch line from left to right as seen by the "observer."

Note that if the branch "line" is actually a circle (as for the van der Pol oscillator [5]), then the first and last branches are also adjacent. In addition to orientation, there is a further n-fold labeling degeneracy corresponding to the n-cyclic permutations of the branch labels.

The second symbol t indicates the torsion of the branch. This is the number of half-twists that occur in the branch during one topological period (the flow from branch line back to branch line). Using the standard convention in linking theory, this number is positive for right-handed crossings and negative for left-handed crossings.

As the branches approach the branch line, they have some ordering before being squeezed together and joined. The third and final symbol j indicates the position of the branch in this ordering. In analogy with the branch line, introduce an *array line* oriented transversely to the branch line and flow direction, so that the index $j = 0, 1, \ldots, n-1$ describes the order in which branches intersect this line. The array line has a natural interpretation as the local stable manifold along which the Birman-Williams projection was carried out. Since there are two possible orientations for this line, there are two possible orderings for the j indices. A conventional choice is to assign the numbers in increasing order as they are encountered along the line of sight from the "observer."

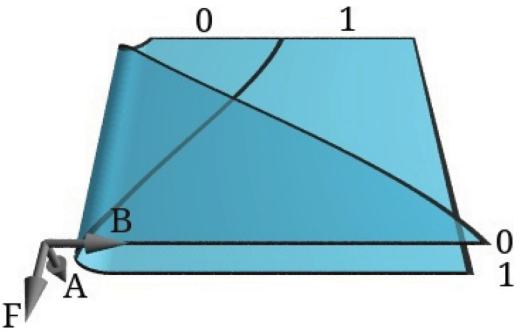

FIG. 1. (Color online) Standard orientation: flow (F) top-to-bottom, branch line (B) left-to-right, and array line (A) front-to-back.

We reiterate that the determination of the first and third indices requires a choice of orientation for the branch line and the array line, respectively. We define a standard orientation as follows: when the flow is downward, the branch line is oriented from left to right and the array line is oriented front-to-back (see Fig. 1). Since the observer could be on either side of the branch-line–flow-direction plane, there are two possible standard orientations. The relationship between these orientations will be discussed in the next section.

Figure 2 shows two distinct mechanisms with identical return maps: the (outside-to-inside) stretch-and-roll-mechanism and the S mechanism. For the stretch-and-roll, branch 0 has zero torsion and connects at the bottom of the array line (position 2), so it is dressed with (0,0,2). Branch 1 has a torsion of 1 and connects at the top, so it is dressed with (1,1,0), and branch 2 has a torsion of 2 and connects in the middle, yielding (2,2,1). The dressing indices for the S mechanism are (0,0,2), (1,1,1), and (2,0,0).

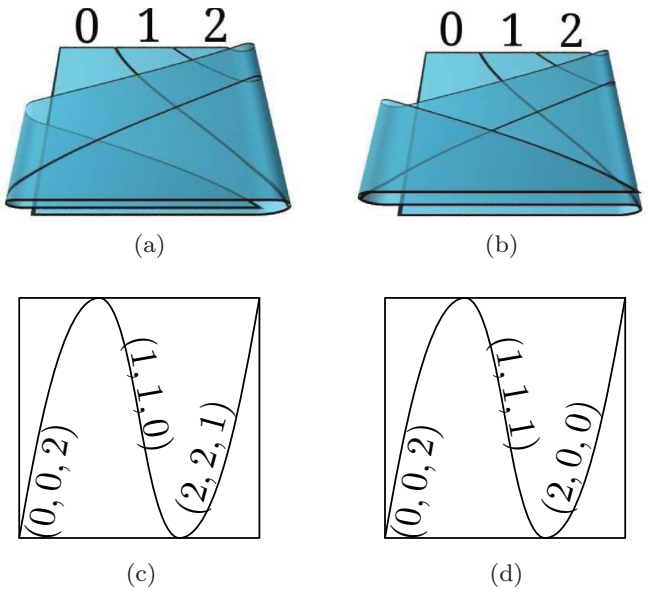

FIG. 2. (Color online) Above: branched manifolds describing the (a) stretch-and-roll and (b) S mechanisms. The flow is from top to bottom, then re-injected at the top (not shown). Below: dressed return maps for the (c) stretch-and-roll and (d) S mechanisms. The dressing indices (i,t,j) label each branch.

III. DEGREES OF FREEDOM

The dressed return maps introduced in the previous section depend on the embedding. Thus, even though the dressings for the two mechanisms in Fig. 2 are distinct, it does not necessarily follow that the two mechanisms are distinct. Here we describe how the dressing transforms with the embedding. This is possible since all of the embedding degrees of freedom are known [9].

Two embeddings that can be smoothly deformed into each other without cutting or self-intersection are called isotopic, and the deformation is called an isotopy. An example of an isotopy is rotating the attractor or, equivalently, moving the location of the observer. Isotopy cannot change the torsions of branches since they are homotopy invariants (linking numbers). Neither can isotopy change the adjacency relations between branches when joined at the branch line. At most an isotopy will change the perspective of the observer and thus the orientations of the branch and array lines. Consider the array line first. A branch encountered first ($j=0$) from one side is encountered last ($j=n-1$) from the other side, and so on. In general, $j \to \bar{j} \equiv n-1-j$. Similarly, the order of the branches is reversed: $i \to \bar{i}$. Finally, we permute the branch labels (carrying the t and j indices) into the standard order. Since there are two possible orientations, isotopy provides a $\mathbb{Z}_2$ (two-fold) freedom. For example, the indices of the stretch-and-roll (Fig. 2) transform as

$$I: \begin{array}{ccc} (0,0,2) \to (2,0,0) & & (0,2,1) \\ (1,1,0) \to (1,1,2) & \not\rightleftarrows & (1,1,2). \\ (2,2,1) \to (0,2,1) & & (2,0,0) \end{array} \tag{1}$$

This shows the transformation of indices (indicated by $\to$), followed by the permutation of the labels (indicated by $\not\rightleftarrows$). In this example, the torsion t_0' of the new branch 0 has the torsion of the old branch $\bar{0}=2$, or $t_0' = t_{\bar{0}} = t_2 = 2$. Similarly, the joining index j_0' of the new branch 0 is the reversed value of the old branch $\bar{0}$, or $j_0' = \bar{j}_{\bar{0}} = 2 - j_2 = 1$. In summary, $(t_i, j_i)' = (t_{\bar{i}}, \bar{j}_{\bar{i}})$, which we write as

$$I: (t_i, j_i) \mapsto (t_{\bar{i}}, \bar{j}_{\bar{i}}).$$

Now consider nonisotopic changes in the embedding. As mentioned previously, this can happen in three ways: knot type, parity, and global torsion. None of the indices is sensitive to knot type, so changing the knot type of the embedding has no effect on the dressed return map.

The parity operation reverses one of the coordinate directions and thus changes the handedness of the embedding. The choice of axis is ultimately immaterial since different choices are related by isotopy. For definiteness we choose the reflection to occur along the branch line, reversing the branch line orientation while preserving the (local) flow and array line. Parity reverses the handedness of crossings, mapping torsions into their negatives: $t \to -t$, and reverses the branch line: $i \to \bar{i}$. Since applying parity twice gives back the original system, this is another $\mathbb{Z}_2$ freedom. Applied to the stretch-and-roll template, using the same notation as Eq. (1), we find

$$P: \begin{array}{ccc} (0,0,2) \to (2,0,2) & & (0,-2,1) \\ (1,1,0) \to (1,-1,0) & \not\rightleftarrows & (1,-1,0). \\ (2,2,1) \to (0,-2,1) & & (2,0,2) \end{array} \tag{2}$$

TABLE I. Transformation properties of the dressing indices under the embedding degrees of freedom: isotopy (I), parity (P), and global torsion (GT). Here, $\bar{j} \equiv n-1-j$ and $m \in \mathbb{Z}$.

	Image under		
Index	I	P	GT
t_i	$t_{\bar{i}}$	$-t_{\bar{i}}$	$t_i + 2m$
j_i	$\bar{j}_{\bar{i}}$	$j_{\bar{i}}$	j_i

The new dressing labels are $(t_i, j_i)' = (-t_{\bar{i}}, j_{\bar{i}})$, or

$$(t_i, j_i) \mapsto (-t_{\bar{i}}, \bar{j}_{\bar{i}}).$$

Finally, a change in global torsion is accomplished by opening the bounding torus along the Poincaré section, adding an integral number of twists to one side of the section, and reconnecting. This operation leaves the section invariant, preserving the flow, branch line, and array line directions, but systematically changes every torsion index (the number of *half* turns) according to $t \to t + 2m$, where m is the integer number of added twists. This provides a $\mathbb{Z}$ (integer-valued) freedom. On the stretch-and-roll template

$$GT: \begin{array}{c}(0,0,2) \to (0,0+2m,2)\\ (1,1,0) \to (1,1+2m,0)\\ (2,2,1) \to (2,2+2m,1)\end{array}, \tag{3}$$

or

$$(t_i, j_i) \mapsto (t_i + 2m, j_i).$$

All together there is a $\mathbb{Z}_2 \otimes \mathbb{Z}_2 \otimes \mathbb{Z}$ freedom in the dressed return map. The three factors correspond to isotopy, parity, and global torsion, respectively. *Two dressed return maps represent equivalent mechanisms if and only if they can be transformed into each other by an element of this group.* Moreover, they are isotopic if and only if the dressings can be mapped into each other using only the first $\mathbb{Z}_2$ subgroup. The action of this group on the dressing labels is summarized in Table I.

These transformation properties can be used to show that the standard and reverse horseshoes (see Fig. 3) are equivalent but nonisotopic mechanisms. An isotopy maps the standard horseshoe indices to

$$\begin{array}{ccc}(0,0,1) & & (0,1,1)\\ & \mapsto & \\ (1,1,0) & & (1,0,0)\end{array},$$

which are not the reverse horseshoe indices, and we conclude that the two are not isotopic. However, the parity operation maps the standard horseshoe indices to

$$\begin{array}{ccc}(0,0,1) & & (0,-1,0)\\ & \mapsto & \\ (1,1,0) & & (1,0,1)\end{array},$$

which are the reverse horseshoe indices. We conclude that these mechanisms are equivalent, differing only by embedding. The equivalence between the direct and reverse horseshoes had previously been observed by Letellier *et al.* [17].

IV. DISTINGUISHING MECHANISMS

The preceding section demonstrated that two mechanisms are equivalent precisely when their dressed return maps can be mapped into each other under the action of a group. Here we introduce an invariant that completely distinguishes any two mechanisms: a mapping exists between two dressed return maps precisely when they have the same invariant.

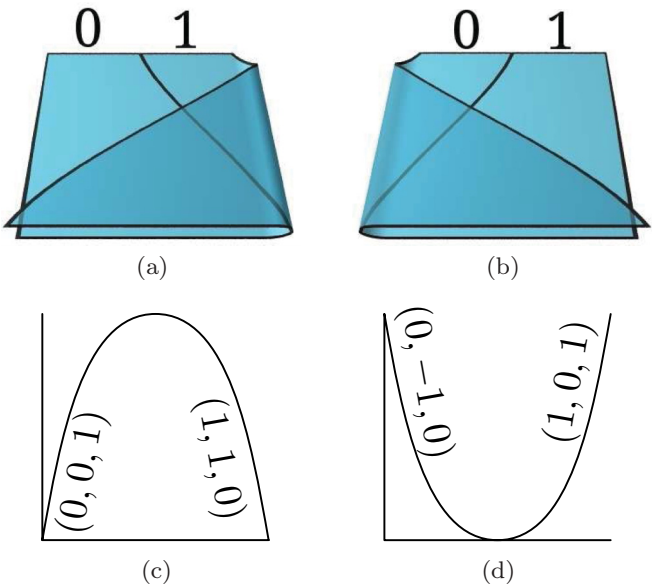

FIG. 3. (Color online) Above: branched manifolds describing the (a) standard and (b) reverse horseshoe mechanisms. The flow is from top to bottom. Below: dressed return maps for the (c) standard and (d) reverse horseshoe. The branched manifolds and dressed return maps differ by parity.

First define the *differential torsion array* ∂t, whose entries are the differences in torsions in adjacent branches,

$$\partial t_i \equiv t_i - t_{i-1} = \pm 1,\ i = 1, \ldots, n-1.$$

This array is manifestly invariant under a change of global torsion since every torsion index transforms by the same fixed quantity, which is then subtracted away. Since an isotopy (I) reverses the branch order, the differential torsion array transforms as

$$I: \partial t_i = t_i - t_{i-1} \mapsto t_{\bar{i}} - t_{\overline{i-1}} = -\partial t_{\overline{i-1}} \equiv -\partial \bar{t}_i,$$

since $\overline{i-1} = \bar{i} + 1$, and we have defined $\partial \bar{t}_i \equiv \partial t_{\overline{i-1}} = \partial t_{n-i}$, which is the reverse of the original array. Parity, in addition to reversing the branches, negates each torsion index ($t \mapsto -t$), so that

$$P: \partial t \mapsto \partial \bar{t}.$$

Next define the *differential joining array* ∂j by

$$\partial j_i = j_i - j_{i-1},\ i = 1, \ldots, n-1.$$

Global torsion has no effect on the joining indices, so ∂j is manifestly invariant under global torsion. Isotopy, in addition to reversing the branch order, reverses the joining index values ($j \mapsto \bar{j}$) so that

$$I: \partial j_i = j_i - j_{i-1} \mapsto \bar{j}_{\bar{i}} - \bar{j}_{\overline{i-1}} = j_{\bar{i}} - j_{\overline{i-1}} = \partial \bar{j}_i,$$

where $\partial \bar{j}_i \equiv \partial j_{\overline{i-1}}$. Parity only reverses the branches, so

$$P: \partial j \mapsto -\partial \bar{j}.$$

TABLE II. Transformation properties of the differential arrays under parity (P), isotopy (I), and the combination $IP = PI$, and where we have defined $\partial\bar{t}_i \equiv \partial t_{\overline{i-1}} = \partial t_{n-i}$.

	Image under		
Array	P	I	IP
∂t	$\partial\bar{t}$	$-\partial\bar{t}$	$-\partial t$
∂j	$-\partial\bar{j}$	$\partial\bar{j}$	$-\partial j$

The transformation properties of both arrays are summarized in Table II.

Both arrays are invariant under global torsion and knot type, so only the $\mathbb{Z}_2 \otimes \mathbb{Z}_2$ freedom of isotopy and parity remains. To define the invariant, first form the combined array $A_0 = (\partial t; \partial j)$. The $\mathbb{Z}_2 \otimes \mathbb{Z}_2$ freedom generates three other arrays: $A_P \equiv PA_0 = (\partial\bar{t}; -\partial\bar{j})$, $A_I \equiv IA_0 = (-\partial\bar{t}; \partial\bar{j})$, and $A_{IP} \equiv IPA_0 = (-\partial t; -\partial j)$. *Define the invariant A by ordering $\{A_0, A_P, A_I, A_{IP}\}$ lexicographically and taking the smallest element.*

This invariant readily distinguishes the stretch-and-roll and S mechanisms presented in Fig. 2. For the stretch-and-roll $\partial t = (1,1)$ and $\partial j = (-2,1)$, so that $A_0 = (1,1;-2,1)$. The other possible arrays are $A_P = (1,1;-1,2)$, $A_I = (-1,-1;1,-2)$, and $A_{IP} = (-1,-1;2,-1)$. Clearly $A_I < A_{IP} < A_0 < A_P$ and the invariant is $A = A_I = (-1,-1;1,-2)$. For the S mechanism $\partial t = (1,-1)$ and $\partial j = (-1,-1)$, and the invariant is $A = A_P = (-1,1;1,1)$. We conclude that the stretch-and-roll and S mechanisms are distinct; there is no diffeomorphism that transforms the stretch-and-roll into the S mechanism.

The stretch-and-roll actually comes in two varieties: outside-to-inside and inside-to-outside. These two are related through the parity operation and thus represent the same underlying mechanism. The dressings and invariants for both stretch-and-rolls and the S mechanism are given in Table III.

As a final example, consider the two double-fold mechanisms shown in Fig. 4. The two folds in Fig. 4(a) are in the same direction, whereas the folds in Fig. 4(b) are in contrary directions. For the first double fold, $A_0 = (1,1,-1;-3,1,1)$ and the invariant is $A_{IP} = (-1,-1,1;3,-1,-1)$, while for the second double fold, $A_0 = (1,-1,-1;-1,-1,3)$ and the invariant is $A_P = (-1,-1,1;-3,1,1)$, hence these are distinct mechanisms.

The stretch-and-roll mechanism is a submechanism of the first double fold, obtained by pruning branch 3. Eliminating this branch removes the last entry in ∂t and ∂j, but the first joining differential changes from -3 to -2 since branch 3 was connected between branches 2 and 0. Hence $A_0 \mapsto (1,1;-2,1)$, which was A_0 for the stretch-and-roll invariant.

TABLE III. Dressings and invariants for the equivalent out-to-in and in-to-out stretch-and-rolls and the inequivalent S mechanism.

System	Dressing (i,t,j)	Invariant
Out-to-in	(0,0,2),(1,1,0),(2,2,1)	$(-1,-1;1,-2)$
In-to-out	$(0,-2,1),(1,-1,2),(2,0,0)$	$(-1,-1;1,-2)$
S	(0,0,2),(1,1,1),(2,0,0)	$(-1,1;1,1)$

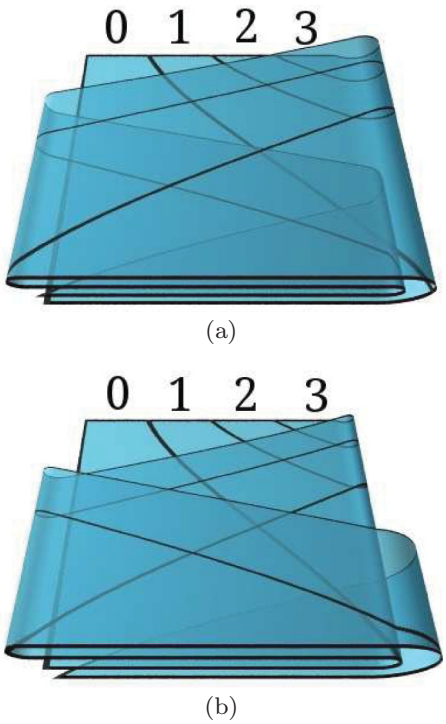

FIG. 4. (Color online) Double-fold mechanisms with the folds in the same direction (a) and in contrary directions (b).

Similarly, pruning branch 3 from the second double fold leaves the S mechanism and $A_0 \mapsto (1,1;-1,-1)$, which is A_0 for the S mechanism.

Alternatively, pruning branch 0 from the first double fold leaves an S-like mechanism, but with an extra half-twist. This is indeed distinct from the S mechanism as the invariant is $A_P = (-1,1;-1,-1)$. Similarly, pruning branch 0 from the second double fold leaves a stretch-and-fold-like mechanism with an extra half-twist, and the invariant is $A_P = (-1,-1;-2,1)$.

The two different three-branch limits of the four branch double-fold templates obtained by pruning an end branch allow a more intuitive understanding of the results of experiments carried out by Used and Martín [18]. The results of these experiments showed templates of both scroll and S types. At the time it was difficult to reconcile these results with the operation of continuous folding of the flow. With the results above, we can now envision a flow evolution beginning with a three-branch template (e.g., 0-1-2) of scroll type, adding a fourth branch (3) to create a template of double-fold type, and then pruning away the first branch, leaving a three-branch template (1-2-3) of S type. Such an evolution is achieved without violating the continuity of the underlying equations.

The invariant array introduced here is simple to compute once the dressed return map has been determined and can differentiate any two mechanisms in genus-1 attractors. We infer that the differential torsion and joining information are sufficient for determining the universality class of a genus-1 attractor. It follows that the entire spectrum of relative rotation rates and linking numbers that characterize a particular representation can be computed from the full dressed return map. This agrees with the analysis in [19].

V. DISCUSSION AND CONCLUSIONS

Chaotic data generated by a three-dimensional dynamical system can be embedded into $\mathbb{R}^3$ in many different ways, each a representation of the same underlying mechanism. To identify this mechanism, we introduced a dressed return map computable from any embedding. We showed that two mechanisms are identical precisely when their dressed return maps can be transformed into each other under the action of a particular group. We then defined an invariant that completely specifies the mechanism by "modding out" this group action. Two mechanisms are the same if and only if they have the same value for this invariant. It is now possible to determine a chaos-generating mechanism in an embedding-independent way. We have worked this out in detail only for genus-1 attractors; the theory for higher genus attractors will be presented in a forthcoming manuscript.

[1] F. Takens, in *Dynamical Systems and Turbulence*, Lecture Notes in Mathematics, edited by D. A. Rand and L. S. Young (Springer-Verlag, New York, 1981), Vol. 898, pp. 366–381.

[2] N. H. Packard, J. P. Crutchfield, J. D. Farmer, and R. S. Shaw, Phys. Rev. Lett. **45**, 712 (1980).

[3] H. D. I. Abarbanel, R. Brown, J. J. Sidorowich, and L. S. Tsimring, Rev. Mod. Phys. **65**, 1331 (1993).

[4] R. Gilmore, Rev. Mod. Phys. **70**, 1455 (1998).

[5] R. Gilmore and M. Lefranc, *The Topology of Chaos: Alice in Stretch and Squeezeland* (Wiley, New York, 2002).

[6] G. B. Mindlin and H. G. Solari, Phys. Rev. E **52**, 1497 (1995).

[7] R. Gilmore, Chaos **17**, 013104 (2007).

[8] N. Romanazzi, M. Lefranc, and R. Gilmore, Phys. Rev. E **75**, 066214 (2007).

[9] D. J. Cross and R. Gilmore, Phys. Rev. E **80**, 056207 (2009).

[10] D. J. Cross and R. Gilmore, Phys Rev. E **81**, 066220 (2010).

[11] D. J. Cross and R. Gilmore, Phys. Rev. E **82**, 056211 (2010).

[12] D. J. Cross, Ph.D. thesis, Drexel University, 2010.

[13] O. E. Rössler, Phys. Lett. A **57**, 397 (1976).

[14] T. D. Tsankov and R. Gilmore, Phys. Rev. Lett. **91**, 134104 (2003).

[15] J. S. Birman and R. F. Williams, Topology **22**, 47 (1983).

[16] J. S. Birman and R. F. Williams, Contemp. Math. **20**, 1 (1983).

[17] C. Letellier, G. Gouesbet, and N. Rulkov, Int. J. Bif. Chaos **6**, 2531 (1996).

[18] J. Used and J. C. Martín, Phys. Rev. E **82**, 016218 (2010).

[19] J. C. Martín and J. Used, Int. J. Bif. Chaos **19**, 3803 (2009).